Maximizing Output Power from Solar Cells/Panels through the Development of an Integrated Voltage Regulator/MPPT Circuit

Joseph O'Connor Sherif Michael Robert Ashton Joseph Madren

Electrical and Computer Engineering Department
Naval Postgraduate School
Monterey, California, United States

***Abstract*—This paper presents the initial results of our research effort to fully integrate a voltage regulator with a Maximum Power Point Tracking (MPPT) circuit in order to harvest maximum power from solar cells or panels. We take a novel approach to emulate the inductor in a buck-boost voltage regulator using a Generalized Impedance Converter (GIC), thereby eliminating the requirement for the grounded inductor which impedes full integration. LTSPICE™ models are developed to compare a traditional "inductive" voltage regulator with a "GIC" voltage regulator, and experimental results are discussed. Component size, switching frequency, and load-matching are optimized to achieve maximum efficiency; however, GIC operational-amplifier power consumption was an obstacle to high-efficiency operation.**

I. Introduction

Photovoltaic solar cells (hereafter "cells") convert incident light to electrical power and have found widespread acceptance as an alternative energy source to carbon fuels. In some applications, cells are connected in series to form panels with sufficient power to charge batteries and run electronic devices. Panels are often connected in both series and parallel to form arrays in order to power bigger loads.

Each cell (panel, array, etc.) has a specific current-voltage operating point where it produces maximum power. The operating point can change due to the fluctuation of temperature and irradiance as shown in Fig. 1 and Fig 2.

For maximum power transfer (MPT) to occur from the source to the load, the characteristic impedance of the source must match the load impedance, which can change. Therefore, directly connecting a source to a load is the least efficient method of power transfer. A better alternative is to insert MPPT circuitry between the source and load to enable MPT through matched impedance as shown in Fig. 3.

Over the last few decades, MPPT has been widely used in solar arrays, panels, and even sub-panels, but the natural progression to "per-cell" MPPT has been inhibited by the cost, size, and power consumption of MPPT circuitry. Recently however, the push to develop efficient, integrated-circuit (IC) voltage regulators has allowed per-cell MPPT to emerge as a feasible concept.

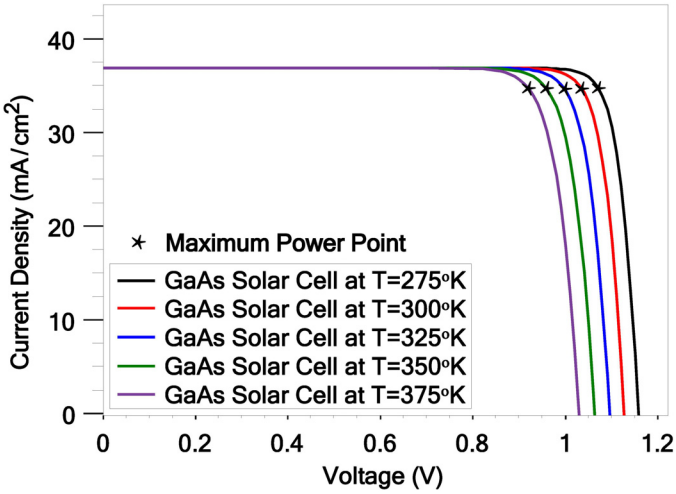

Fig. 1. Maximum power point varies with solar cell temperature.

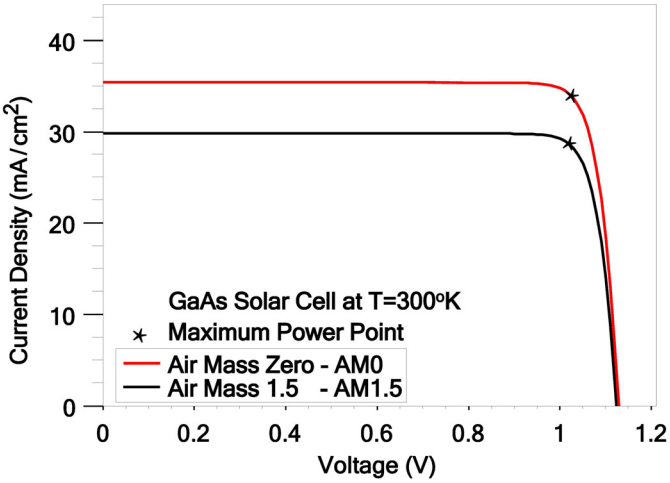

Fig. 2. Maximum power point varies with solar irradiance.

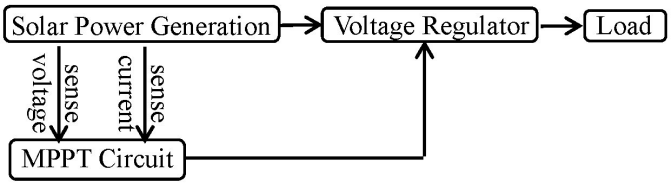

Fig. 3. Solar Power Generation with MPPT Circuit and Voltage Regulator.

The main roadblock to IC MPPT is the discrete inductor found in traditional, switching voltage regulators. Switched-capacitor (SC), monolithic inductive (MI), and system-on-a-chip (SiC) regulators attempt to circumvent the inductor problem: SC regulators eliminate the inductor, while MI and SiC regulators incorporate the inductor during or after chip production using dedicated, post-processing technology. All three approaches show a tradeoff between power density and efficiency [1]-[3].

This work seeks another path towards on-chip voltage regulation by implementing a Generalized Impedance Converter (GIC) in place of the inductor in a buck-boost voltage regulator (hereafter "voltage regulator"). The paper is organized as follows: Ch. II explains the concept of emulated inductance; Ch. III explains how a GIC voltage regulator works and presents LTSPICE models for comparison; Ch. IV discusses experimental results.

II. Emulating Inductance Using a GIC

The GIC shown in Fig. 4 has been around for decades and is often used to emulate inductance in signal filtering because it permits inductance to be realized on a chip. The equivalent output impedance of the GIC can be derived as

$$Z_{GIC} = \frac{Z_1 Z_3 Z_5}{Z_2 Z_4}. \tag{1}$$

If impedances are chosen such that Z_1, Z_3, Z_4, and Z_5 are resistors, and Z_2 is a capacitor, the output impedance becomes

$$Z_{GIC} = \frac{R_1 R_3 R_5}{\frac{1}{j\omega C_2} R_4} = \frac{R_1 R_3 R_5 j\omega C_2}{R_4}. \tag{2}$$

Lastly, if resistor values are combined to an equivalent resistance, R_{eq}, (2) becomes

$$Z_{GIC} = j\omega(C_2 R_{eq}) = j\omega L_{eq}, \tag{3}$$

which is the equivalent impedance of the GIC. Note that for chip design, the resistors can be replaced with bi-linear switched capacitors to enable integration on a chip and reduce power consumption.

III. Inserting the GIC into a Buck-Boost Voltage Regulator

We inserted the GIC into a voltage regulator (hereafter "voltage regulator") to replace the grounded inductor as shown in Fig. 5. GIC component values were selected to emulate a 125mH inductor; inductance was verified in a single-pole high-pass RL filter in LTSPICE as shown in Fig. 6. We marked the cutoff frequency on a Bode plot and calculated inductance using

$$f_{cutoff} = \frac{R}{\omega L}, \tag{4}$$

where R is the series resistance of the filter, ω is the angular frequency in radians per second, and L is the inductance.

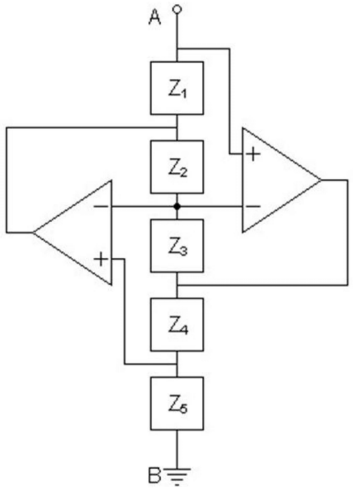

Fig. 4. Generalized Impedance Converter.

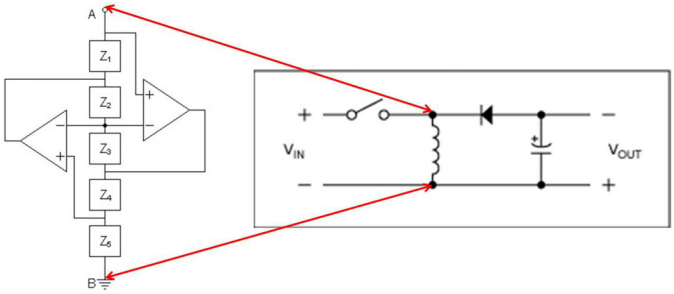

Fig. 5. GIC inserted into a buck-boost voltage regulator.

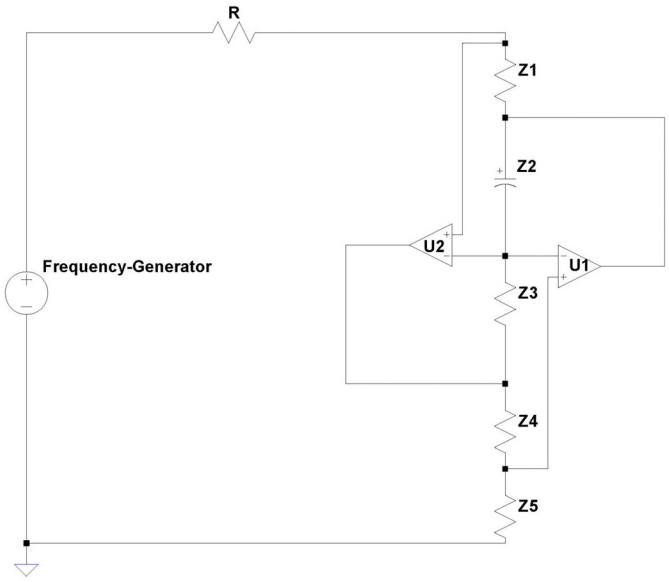

Fig. 6. Single-pole, high-pass, RL filter modeled in LTSPICE.

Then we developed two models in LTSPICE using ideal components. The first model, shown in Fig. 7, was a standard voltage regulator that utilized a 125mH inductor. The second model, shown in Fig. 8, employed the GIC circuit in place of the inductor. All other components were identical and the pulse-width-modulation (PWM) switching frequency was held constant. The "GIC" voltage regulator performed identically to the "traditional" regulator when both operational amplifiers (OPAMP) operated in their active regions (unsaturated). Active region operation was achieved by adjusting the input voltage, duty cycle, and load impedance. Output (load) voltage waveforms for both voltage regulators are shown in Fig. 9 and Fig. 10.

Next, we replaced "ideal" component models in the "GIC" voltage regulator with commercially available component models available in LTSPICE. Many components were evaluated to maximize efficiency and power density. Synchronous switching was employed via the LTC1982 gate driver, and low-power-density NDC7002 MOSFETS were used. A low input voltage of 1.8V and a resistive load of 175Ω limited OPAMP current to <120mA to prevent saturation. The low input voltage also enabled a reduction of the +/-Vcc OPAMP supplies which minimized GIC power consumption. The optimized circuit is shown in Fig. 11.

We operated the voltage regulator model in continuous conduction mode (CCM) at duty cycles of 40%, 50%, and 60%. Output voltage waveforms are shown in Fig. 12. An efficient voltage regulator operating at 50% duty cycle should produce and output voltage that is nearly the same as the input voltage (1.8V); however, we note from Fig. 12 that the output voltage is only ~1V which suggests excessive power loss in the circuit. Analysis showed that the OPAMPs consumed too much power (via the +/-Vcc inputs) for efficient operation of the circuit.

IV. Expirmental verification

Model results were verified using a commercial, on-chip, voltage regulator with an external, grounded conductor. The regulator was placed on a circuit board next to a GIC designed for the same inductance as shown in Fig. 13. GIC inductance was verified by inserting the GIC into a high-pass filter, measuring the cutoff frequency, and calculating the inductance using (4). A linear power source provided +/-Vcc to the OPAMPs; another source provided voltage to the commercial voltage regulator. The setup enabled the inductor to be removed from the voltage regulator and the GIC inserted in its place to make comparisons and take measurements.

Experimental measurements confirmed the LTSPICE model predictions that OPAMP power consumption was excessive and prohibited high-efficiency operation. Additionally, the OPAMPs saturated when load current exceeded 100mA.

V. Conclusion

Under optimal conditions (i.e. matched components, MPT, unsaturated OPAMPs) GIC power consumption exceeded the power delivered by the source. We conclude that since the GIC cannot store and release energy, the OPAMPs must source or sink current to maintain load current. Conversely, a physical inductor can store energy from a source, then deliver the energy to the load through the expansion and contraction of a magnetic field. Therefore, although the GIC performed well in the voltage regulator and emulated inductance as expected, OPAMP power consumption makes the application impractical for MPPT and other circuits that require high-efficiency performance.

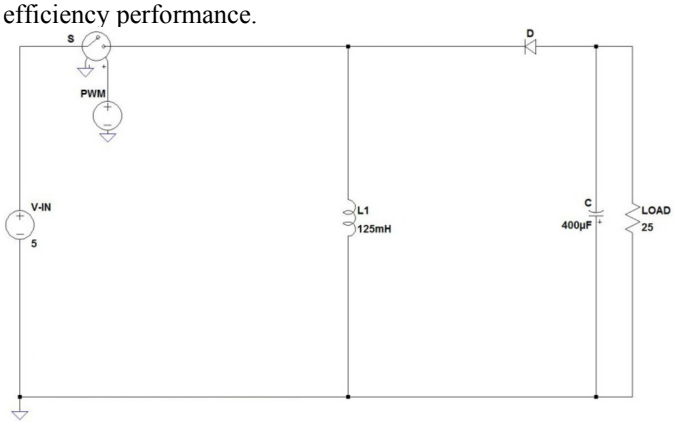

Fig. 7. Voltage regulator utilizing a physical inductor model in LTSPICE.

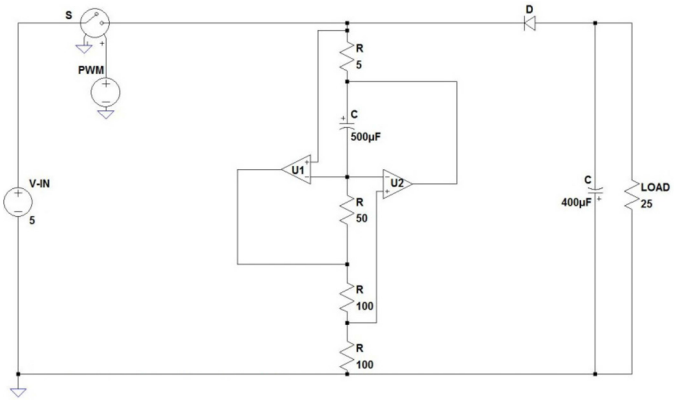

Fig. 8. Voltage regulator utilizing a "GIC" inductor model in LTSPICE.

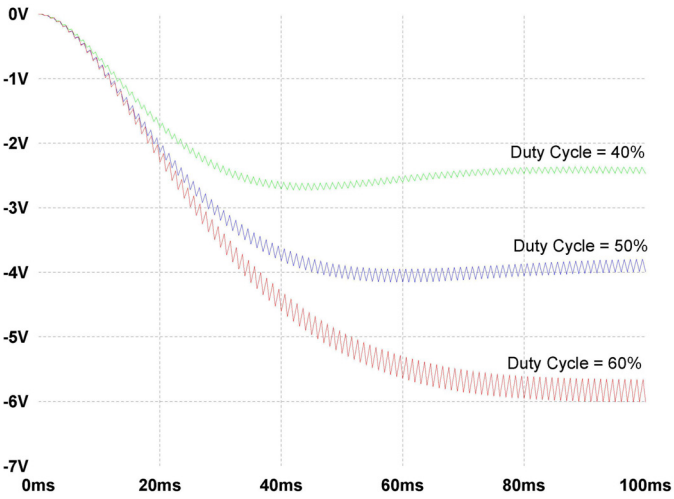

Fig. 9. Output (load) voltage waveforms for a voltage regulator utilizing a physical inductor model in LTSPICE.

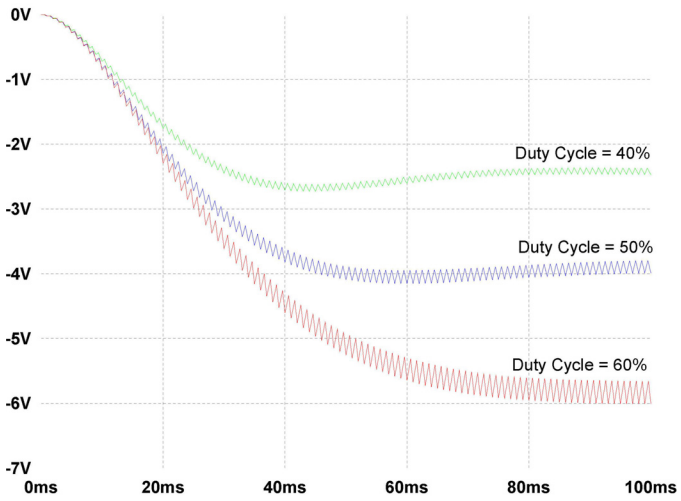

Fig. 10. Output (load) voltage waveforms for a voltage regulator utilizing an ideal "GIC" inductor model in LTSPICE.

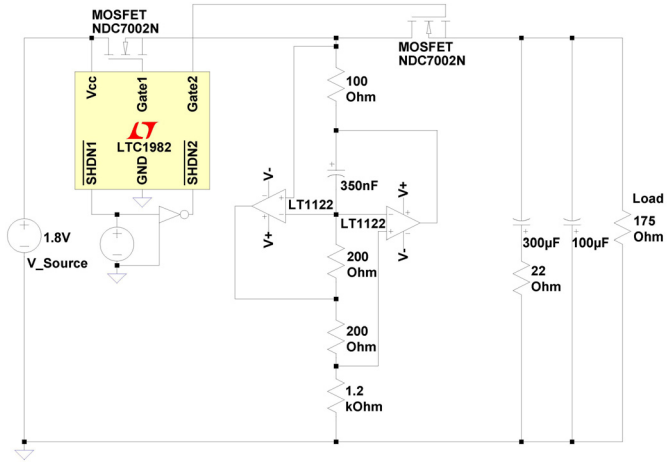

Fig. 11. Voltage regulator with "GIC" inductor utilizing commercially available component models in LTSPICE.

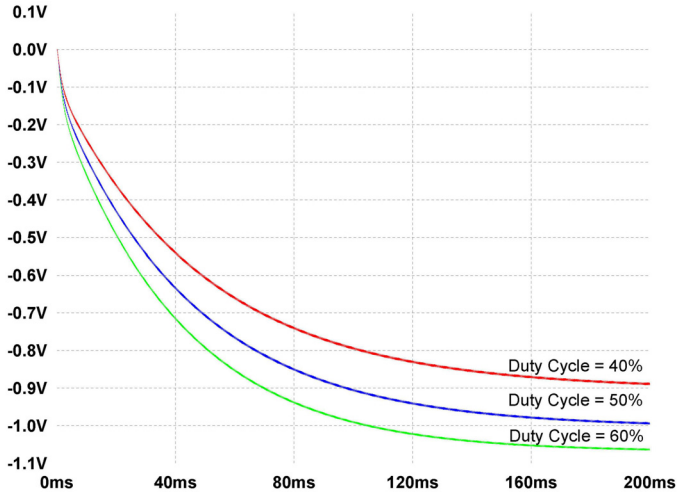

Fig. 12. Output (load) voltage waveforms for a "GIC" voltage regulator utilizing commercially available component models in LTSPICE.

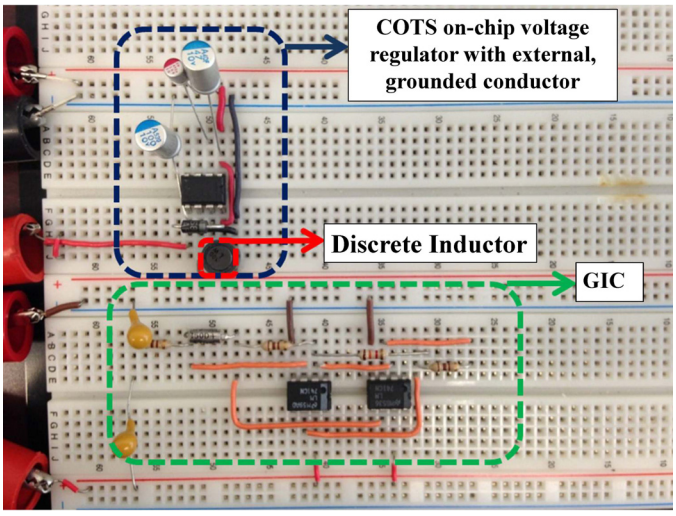

Fig. 13. Experimental setup of a commercial-off-the-shelf (COTS) voltage regulator with an external, grounded inductor. The GIC was inserted in place of the inductor to compare performance.

REFERENCES

[1] G. Villar-Pique, H. Bergveld, and E. Alarcon, "Survey and benchmark of fully integrated switching power converters: switched-capacitor versus inductive approach," in *IEEE Transactions on Power Electronics,* vol. 28, no. 9, pp. 4156-4167, Sep 2013.

[2] M. Makowski and D. Maksimovic, "Performance limits of switched-capacitor DC-DC converters," in *Proc. IEEE Power Electron. Spec. Conf.*, 1995, pp. 1215-1221.

[3] H. Meyvaert, T. Van Breussegem, and M. Steyaert, "A monolithic 0.77W/mm^2 power dense capacitive DC-DC step-down converter in 90nm bulk CMOS," in *Proc. IEEE 37th Solid-State Circuits Conf.*, Helsinki, 2011, pp. 483-486.